Original Article

Institution of MECHANICAL ENGINEERS
Journal of MECHANICAL ENGINEERING SCIENCE

Proc IMechE Part C:
J Mechanical Engineering Science
2019, Vol. 233(16) 5547–5555

DOI: 10.1177/0954406219856028
journals.sagepub.com/home/pic
SAGE

# Analysis and validation of femur bone data using finite element method under static load condition

**S Mathukumar[1], VA Nagarajan[2] and A Radhakrishnan[3]**

## Abstract

Humans face bone fracture when they unfortunately met an accident, which requires timely medical attention for healing and repairing the fractured bone; otherwise that paralyzes their life. 3D modeling technique with computational method is very helpful at the side of doctors for healing and repairing the damaged bones. Fractional bone healing is one of the natural processes, which regain the mechanical reliability of the bone to a limited level of failures. The relationship between the biology and mechanics has introduced a new branch namely biomechanics. Various biomechanics models were used to identify the fracture for different patients and helps in the fracture treatment. The aim of this work is to find out the high stress concentration area of the femur bone, which has been extracted as image from computer tomography scanner. The retrieved noise-free femur bone image is tested by the static load condition with the help of the finite element analysis. The result obtained from the testing of different loads has been compared with the existing literature. It is found that the femur bone has tensile and compressive stress, and the neck area of the femur is at a very high stress concentration. The outcome of this work is much supportive to orthopedic surgeons in femur surgery and bone prosthesis by avoiding experiments on femur bone.

## Keywords

Femur bone, prosthesis, biomechanics, finite element method

Date received: 4 February 2019; accepted: 16 May 2019

## Introduction

Three-dimensional finite element (FE) modeling is widely used to generate reliable subject-specific FE model using computed tomography (CT) data that accurately predict information about bone morphology and tissue density. The mechanical behavior of the long bones has been explained by the FE modeling, and these long bones are scanned by CT scan. In this study, 3D image of the human femur bone has been formulated, and also the data related to the hip contact forces on the femur bone, which are created during walking and standing, are used to inquire the behavior of the femur bone. The results which are received by FE modeling are compared with experimental studies. These results are used for orthopedic surgeon to interpret the biomechanical demeanor of the femur bone and also used in surgeries and prosthesis of bone. CT scan data are widely used to make realistic investigations on the mechanical behavior of bone structures using FEA to determine the equivalent Von Mises stress and strain. Analysis of these models will provide data unavailable at this time to orthopedic surgeons, engineers, and researchers of human orthopedic. Being an important structure femur serves two distinct functions: it acts as a supporting structure allowing the weight of the upper body to be transferred from the hip joint to the knee joint, and it also acts as a stiff structure about which muscles act to facilitate movement at both the hip and knee joints. Structural weakness and fracture is the neck of the femur which women usually suffer mostly occurring at the age of 65 or above. Due to the extreme force on femur, fracture of the shaft occurs. The structure of the femur has two types: one is cortical or compact bone. This bone is a dense outer layer which prevents bending. Another one is cancellous or

[1]Faculty of Mechanical Engineering, Ponjesly College of Engineering, Nagercoil, India
[2]Faculty of Mechanical Engineering, University College of Engineering, Nagercoil, India
[3]Faculty of Information Technology, University College of Engineering, Nagercoil, India

**Corresponding author:**
S Mathukumar, Ponjesly College of Engineering, Nagercoil, Thuckalay, Tamil Nadu 629175, India.
Email: smathukumar@gmail.com

spongy which is an inner portion of the mature bones, and it is used to resist compression and dislodge themselves along the direction of functional pressure. Femur bone was selected for modeling and analysis because it is the longest, strongest, and heaviest in the whole human body. Early examinations of osteoporosis can be improved by FEA of bones scanned by quantitative CT (QCT).[1] The QCT reveals the FE models of the proximal femur based on the realistic material which can exactly predict the patient's specific bone strength in vivo.[2] The 3D FE modeling is commonly used to generate reliable subject-specific FE model using CT data. The CT data exactly predicts the information about tissue density and the bone morphology, and FEA predicts the mechanical behavior of bone structures.[3]

The complex micro architecture of the trabecular bone within the proximal femur exhibits anisotropic mechanical behavior, and it is highly difficult to resolve by clinical resolution and therefore it is unavailable in vivo. Isotropic property of human femur bones, particularly the cortex region, was already reported.[5] Based on this study, FE analysis was made. According to this, the current work is executed by considering the isotropic property of the cortex portion of human femur bones. Therefore, numerous studies have been done to create isotropic FE models of the proximal femur bone;[4–11] conversely, there are few agreements in the resulting outcome or the optimal approach which are attributed to a deficiency of validation study which are done by experimental on anisotropic. The proximal femur can be improved by the properties of isotropic material which are highly appropriate of translating this modeling technique into clinical practice. For studying the mechanical behavior structures, the FE method has been highly recognized as the useful tool,[12] and computerized tomography has supported to FE modeling of bone structures.[13]

The precise quantitative information on bone geometry which is related to the bone mechanical properties can be provided by CT image. The basic step in model generation is to assign the bone material properties to FE meshes based on CT data. Currently, the information provided by the CT data for the subject, particularly FE modeling, is used as a tool for the numerical analysis of the biomechanical behavior of human bones.[14–17] The FE analysis demonstrated that the stress distribution of bone is related to the mechanical properties that is from bone tissue.[18,19] FE models can also help in the understanding of femur behavior under different load conditions, regardless of the need of experiments.[27]

## Materials and methods

### *Specimen and experimental testing*

The experiment has been published with the description which are detailed[20] to carry out to decide the high stress concentration of femur bone by experimental analysis and are highly responsible for damages and fractures.

Under physiological load conditions, experimental work is analyzed for the behavior of the femur bone. By using an Electronics Universal Testing machine, quasi static load is applied. The electrical resistance strain gauge and mountings are selected properly on bones' irregular surface area. The fracture in the femur happens due to large force or something wrong with the bone. The frequent causes of femur fractures in patients include falls from height and car accidents, weakened bone by osteoporosis, tumor, or some infection can also responsible for the fracture of femur in patients. Four proximal femur fractures are commonly referred as hip fractures namely (1) femoral head fracture, (2) femoral neck fracture, (3) inter trochanteric fracture, and (4) sub-trochanteric fracture. Proximal femur which means the upper third of the human femur bone includes femoral head, greater trochanter, femoral neck, and upper portion of the femoral stem. The narrowed region called femoral neck is present below the femoral head. The cortical bone, which has higher material density, is present in the outer shell of the bone. The relatively soft, sponge-like bone called trabecular bone is inside the hard cortical shell. The exact position of the bone and strain gauges in this experiment is clearly shown in Figure 1 namely (1) neck inferior, (2) neck superior, (3) shaft lateral, and (4) shaft medial. Strain gauges 3 and 4 are positioned at 134 mm for shaft lateral and 214 mm for shaft medial, respectively, from the femoral head.[30] The positions 1, 2, 3, and 4 were chosen,[28,29] where the probability of fracture in the femur bone is high.

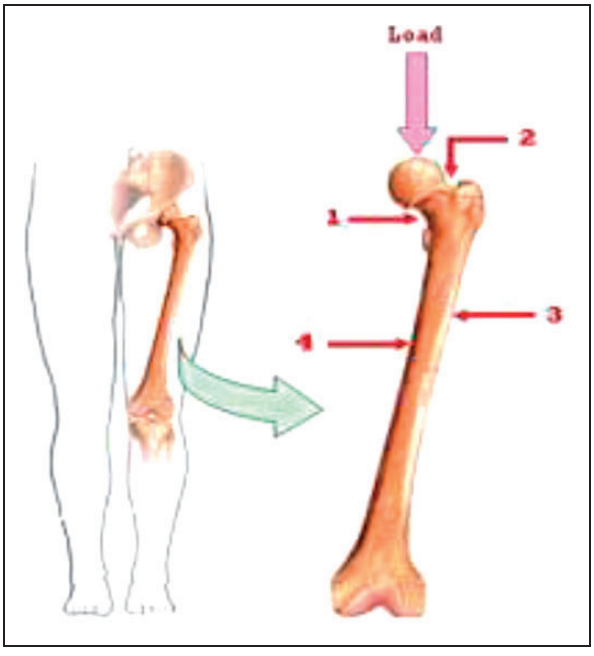


**Figure 1.** Actual position of the femur bone and strain gauges.

The bone sample that comes across an embalmment process is the common method of preserving human bone specimens. To prevent the decomposition of bone structures, the bone is chemically fixed with formaldehyde. The human bone is highly heterogeneous and nonlinear in nature and therefore inherent inhomogeneous and anisotropic nature of bone tissue is still under active research. This method is effective for measuring external strains at the critical location known for fracture initiation and is experimentally validated. The femur bone density value widely used by the different researchers is 2080 kg/m$^3$. The Young's modulus for cortical bone is evaluated according to the functional representation of the density. Hence, different researchers have used the Young's modulus value 14,200 MPa. As the material is nonlinear and heterogeneous, the Poisson's ratio also has different values for different researchers. The commonly taken value of cortical bone is 0.3.[22]

## Femur model extracted from CT data

Femurs were scanned by 16-row MD-CT scanner. In this scanner, human legs were placed in a position and compared to the position used in the viva exam of proximal femur and pelvis. The thickness of the slice was 0.75 mm. The setting was 120 kVp and 100 mAs, a $512 \times 512$ pixel image matrix, a field of view of 100 mm, and inplane spatial resolution was approximately 0.25 mm$\times$ 0.25 mm using a high spatial resolution reconstruction algorithm. The reference phantom was used to scan all femoral bone portion of the leg. The reference phantom consists of two density phases, a 0 mg hydroxyapatite/cm$^3$, and a 200 mg hydroxyapatite/cm$^3$ phase representing the water like and bone like parts of the phantom, respectively. The basic steps for analyzing the femur bone are shown in Figure 2.

Image processing software (3D Doctor) is used for creating the femur bone model and the human internal organ model. The MT-CT scanner was used for scanning the femur bone, and the CT images were used for generating the FE model. Once the scanning is over with the help of CT scan, DICOM files are created. DICOM files are converted into image files with the help of 3D-Doctor software. After opening the DICOM folder, the required image slice will be obtained with help preview. The scanned image has a different number of slices with six image series. After the slices are obtained from the main series, the next step is to trace the femur bone with the help of interactive segment command. The mask operation has to be carried out after the completion of the segmentation part using a Recursive Gaussian filter, that is used to reduce the detailed levels and image noise. Before performing smoothing operation to grow the

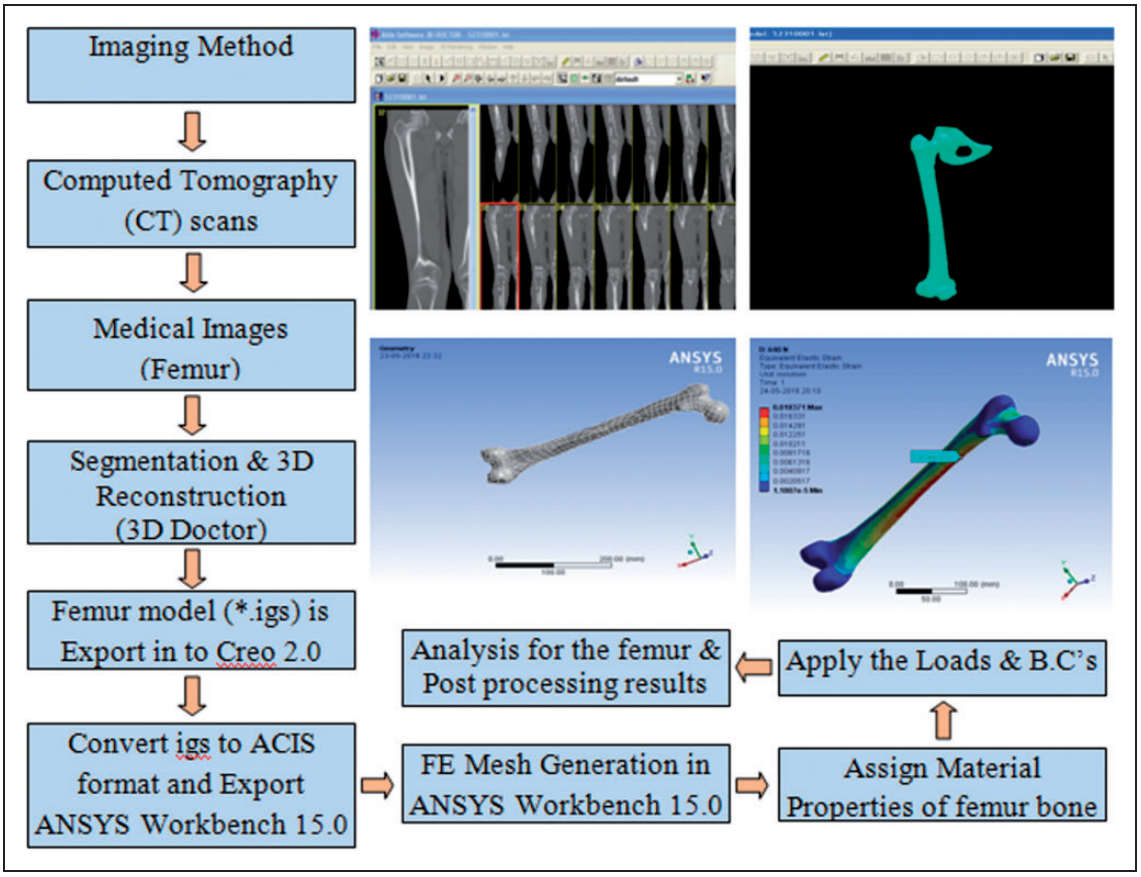


**Figure 2.** Steps for analyzing the femur bone.

mask of a cortical region, before performing smoothing operation to grow the mask of a cortical region, the morphological data filter was applied to the implication of data loss. Hence, cortical and cancellous region masks' Gaussian sigma of 2.5 (cubic values) is applied. Third and fourth phase of modeling depends upon the polygonal model and non uniform rational B spline surfaces. This denotes the border of the inner medullary cavity and the cortical of the femur. The outer surfaces were produced by 3D CAD features, and inside of the femur is split into zones corresponding to regions such as proximal and distal regions. By the use of advanced modeling features in CREO 2.0, the construction of 3D zones was performed. After the construction of 3D zone, the image is stored in ACIS format and that is shown in Figure 3. The ACIS format is suitable for export files to ANSYS software for better compatibility.

## FE model

FE analysis is a mathematical tool, which is used to simplify the complex situations into a number of discrete, smaller problems, individually, and combined to give a proper solution to the complex problem. The work is carried out by dividing the geometries which are complex into a set of small simplexes in the shape of tetrahedral in 3D or triangles in 2D, known as a mesh. The results obtained from the large set of simultaneous equations are used to give the solution of the domain (object) of interest. The specific points are called nodes in which each element is interconnected. The surface mesh generated from the data based on the geometry of a femur is shown in Figure 4. The volume mesh inside the femur is made of triangular elements. Based on in-house programs developed for femurs,[23,24,26,27,29] the automatic 3D reconstruction of the metatarsal geometry from QCT scans and p-version FE meshes was generated. By keeping the fixed mesh and increasing the polynomial degree of the approximated solution, the p-version of the FE method convergence is realized.

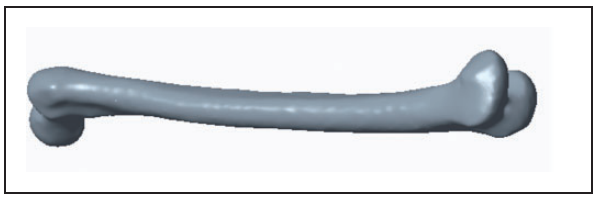

**Figure 3.** ACIS format of femur bone model.

### *Boundary conditions applied to the FE model*

The boundary conditions are applied to the femur during the remodeling analysis. Similar to the walking movement, the femur was distally fixed, and three simultaneous load and their corresponding reactions were considered. The load corresponding to the reaction force of the femoral head and the abductor muscle force takes place when the foot touches the floor.[25] The femur bone was analyzed in the standing posture. Material properties and boundary conditions are initially applied before the different load on the femur bone under static condition is applied. The different loads applied on the femur bones are 490 N (50 kg), 540 N (55 kg), 588 N (60 kg), and

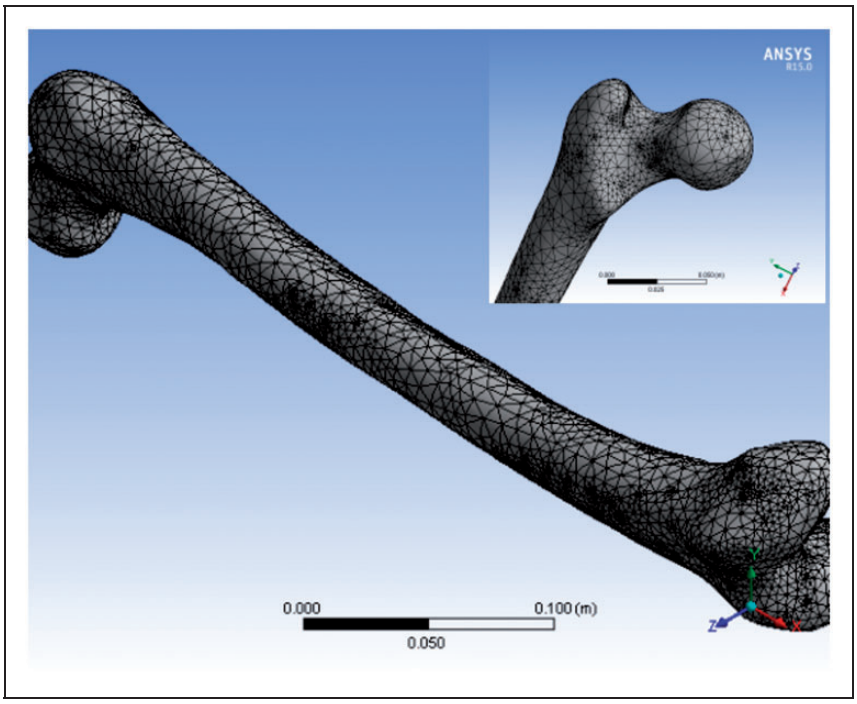


**Figure 4.** Meshing image of femur bone model.

640 N (65 kg) in the experiment and results are obtained.[21] Boundary conditions applied to the femur model are shown in Figure 5.

Various loads were applied to the femoral head by keeping the medial condyle as fixed, and strain gauge was applied at positions 1, 2, 3, and 4. The gauged positions were given in Figure 1.

## Comparison between FE model and experimental testing

Stress and strain predicted by FE models were correlated with the experimental results. Stress and strain were measured from the experiment for the four positions of the strain gauges in which the force is applied[21] and subsequently compared to the FE stress and strain of the same positions.

Figure 6 shows the strain value, and the error obtained is lesser for neck inferior and neck superior and higher for shaft lateral and shaft medial. Figure 6 shows the 490 N load, and the neck inferior and neck superior position has the higher stress value when compared with shaft lateral and shaft medial. The error obtained when compared to the results of FEA is less than 2%. At a static load of 540 N, strain values were obtained from different locations of the bone. Figure 6 shows the 540 N load, and the neck inferior and neck superior position has the higher stress value when compared with shaft lateral and shaft medial. The error percentage obtained in most of the

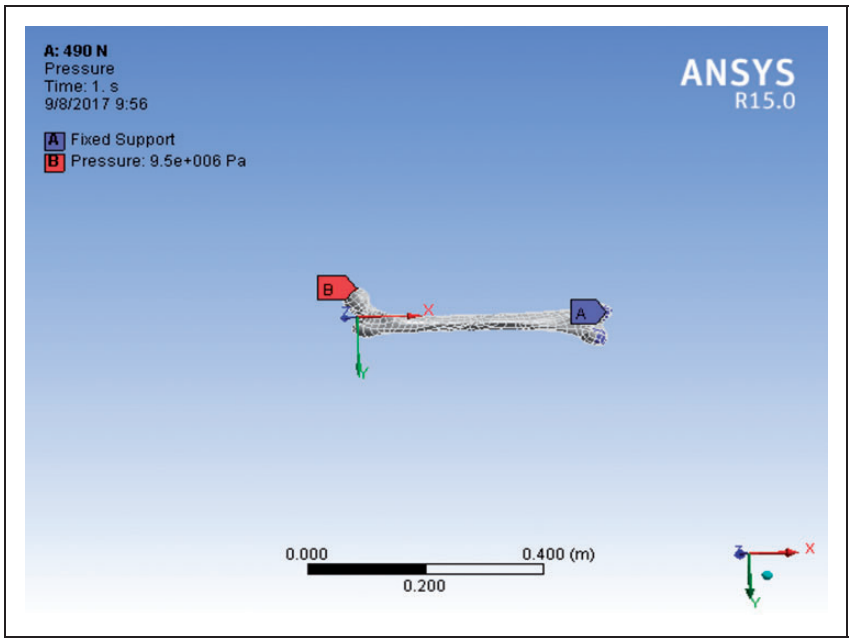


**Figure 5.** Boundary conditions applied on the femur bone.

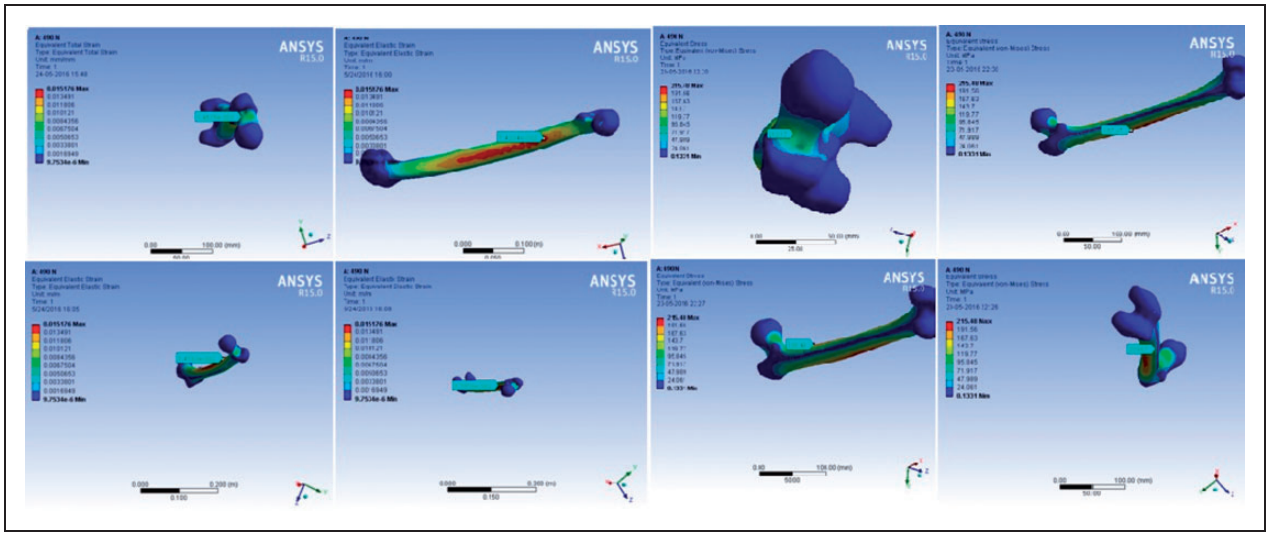


**Figure 6.** Stress and strain result of deformed femur bone under 490 N.

cases is less than 2. Figure 6 shows the value of strain in different locations of the bone under the static load of 588 N. Figure 6 shows the 588 N load, and the error obtained when the results of FEA are around 6% for neck inferior, shaft lateral, and less than 3% for neck superior and shaft medial. Figure 6 shows the value of strain in different locations of the bone under the static load of 640 N. Figure 6 shows the 640 N load, and neck inferior and neck superior position has the higher stress value when compared with shaft lateral and shaft medial. Figure 6 shows the 640N load, and neck inferior and neck superior position has the higher stress value when compared with shaft lateral and shaft medial, for which the percentage of errors are minimum.

Figure 6 shows the stain value, and the error obtained is less than 5% for loads (540, 588, and 640 N) and higher in 490 N.

## Results of experimental and FE analysis

The FE analysis and experimental results were compared and listed in Table 1. Stress and strain values for all the position of the femur bone showed good match with FEA results, and a small deviation is also observed.

Comparison of stress and strain experimental results with FEA results based on different strain gauge positions is given in Figures 7 and 8.

## Discussion

The mechanical behavior like stress and strain of femur bone was predicted by FE model and correlated with the experimental results. The experimental results obtained from the reference and FE Analysis data are given in Table 1. It revealed the relationship of load and stress at different strain gauge positions. Various loads such as 490, 540, 588, and 640 N were applied to analyze the stress and strain results. At these loads, FEA result of stress and strain values was comparable with the experimental results, and only minimum deviations are observed between them. In Figure 7, for strain gauge position 1, a linear increase in stress values corresponding to the increased load was observed. Experimental and FEA results almost matched with each other when the errors obtained are very less, and the variations are only marginal. For strain gauge position 2, as the load values were increased, the stress also increased for both experimental and FEA results, and the errors obtained between them are very less.

FEA data for strain gauge position 3 were compared to the experimental values reported for the stress and strain properties. An increase in stress till 540 N was observed, and there was a gradual decrease till 640 N, and the error percentage for the FEA data in comparison with the experimental values is very less. For strain gauge position 4, the stress values of experimental results increased till 540 N, while there was a slight decrease till 640 N. As the loads were increased, corresponding stress also increased, and the errors observed are very less.

In Figure 8, strain gauge position 1, the experimental values of strain were stable up to 540 N and then increased till 640 N. In FEA results, as the loads were increased, strain also increased, and the errors obtained values are very minimum. For strain gauge

**Table 1.** Comparison of Stress and Strain Experimental results with FEA results.

| | | | Stress | | | Strain | | |
|---|---|---|---|---|---|---|---|---|
| | Strain gauge position | Load (N) | Exp. result ($N/mm^2$) | FEA result ($N/mm^2$) | % of error | Exp. result | FEA result | % of error |
| Reading 1 | 1 | 490 | 213 | 213.17 | 0.079 | 0.015 | 0.01457 | 2.86 |
| | 2 | | 213 | 209.67 | 1.56 | 0.015 | 0.01420 | 5.33 |
| | 3 | | 184.6 | 180.49 | 2.22 | 0.015 | 0.01410 | 6.00 |
| | 4 | | 184 | 187.47 | 1.85 | 0.015 | 0.01390 | 7.33 |
| Reading 2 | 1 | 540 | 213 | 223.41 | 4.65 | 0.015 | 0.01558 | 3.72 |
| | 2 | | 227.2 | 224.27 | 1.3 | 0.016 | 0.01520 | 5.00 |
| | 3 | | 184.6 | 187.45 | 1.5 | 0.013 | 0.01285 | 1.15 |
| | 4 | | 198.8 | 195.38 | 1.7 | 0.014 | 0.01424 | 1.68 |
| Reading 3 | 1 | 588 | 227.2 | 242.91 | 6.46 | 0.016 | 0.01634 | 2.10 |
| | 2 | | 241.4 | 235.6 | 2.40 | 0.017 | 0.01642 | 3.41 |
| | 3 | | 198.8 | 187.1 | 5.88 | 0.014 | 0.01333 | 4.78 |
| | 4 | | 198.8 | 199.11 | 0.01 | 0.014 | 0.01452 | 3.58 |
| Reading 4 | 1 | 640 | 241.4 | 254.2 | 5.03 | 0.017 | 0.01769 | 3.90 |
| | 2 | | 255.6 | 254.33 | 0.04 | 0.018 | 0.01741 | 3.27 |
| | 3 | | 213 | 217.38 | 2.01 | 0.015 | 0.01493 | 0.04 |
| | 4 | | 213 | 213.82 | 0.03 | 0.015 | 0.01497 | 0.02 |

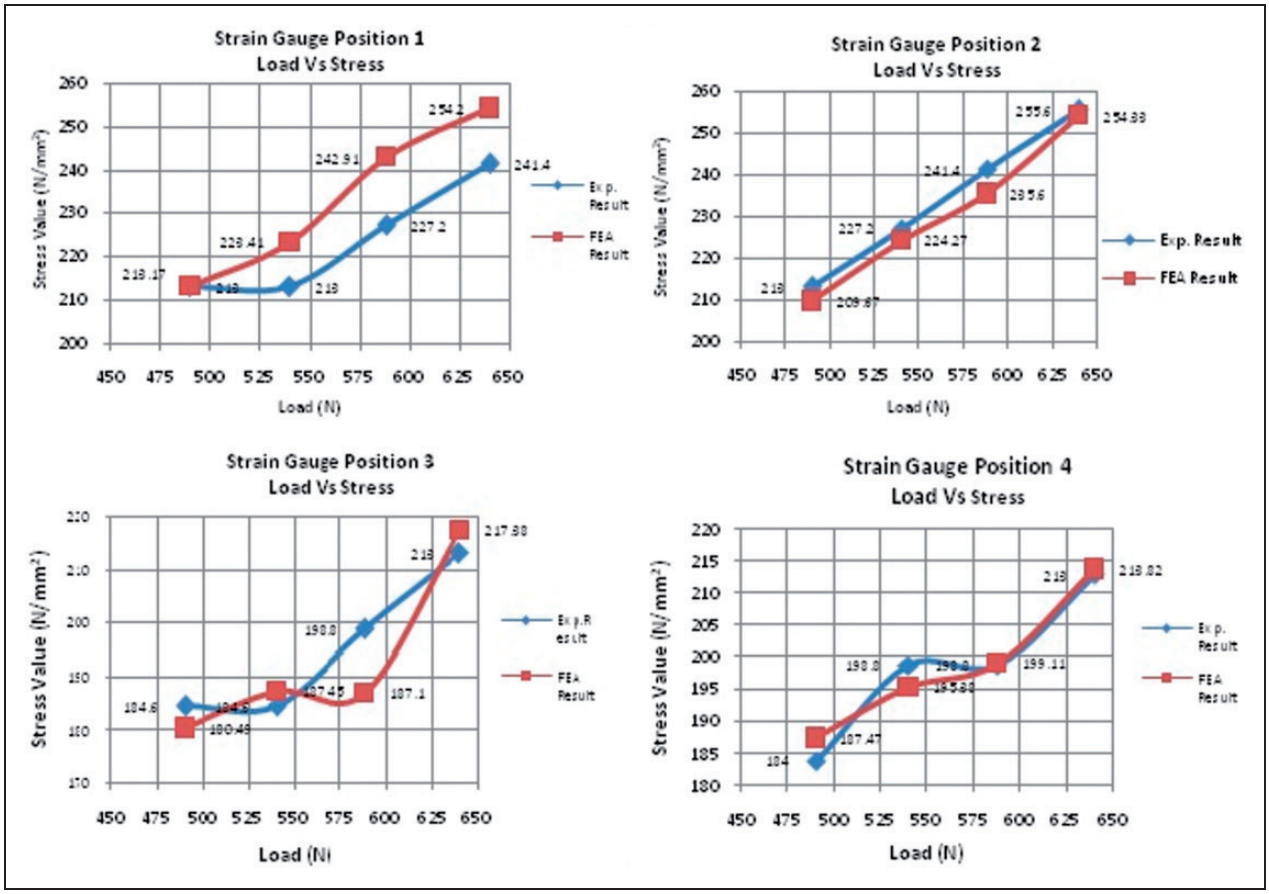


**Figure 7.** Comparatives between stress value for experimental and FEA results based on strain gauge positions.

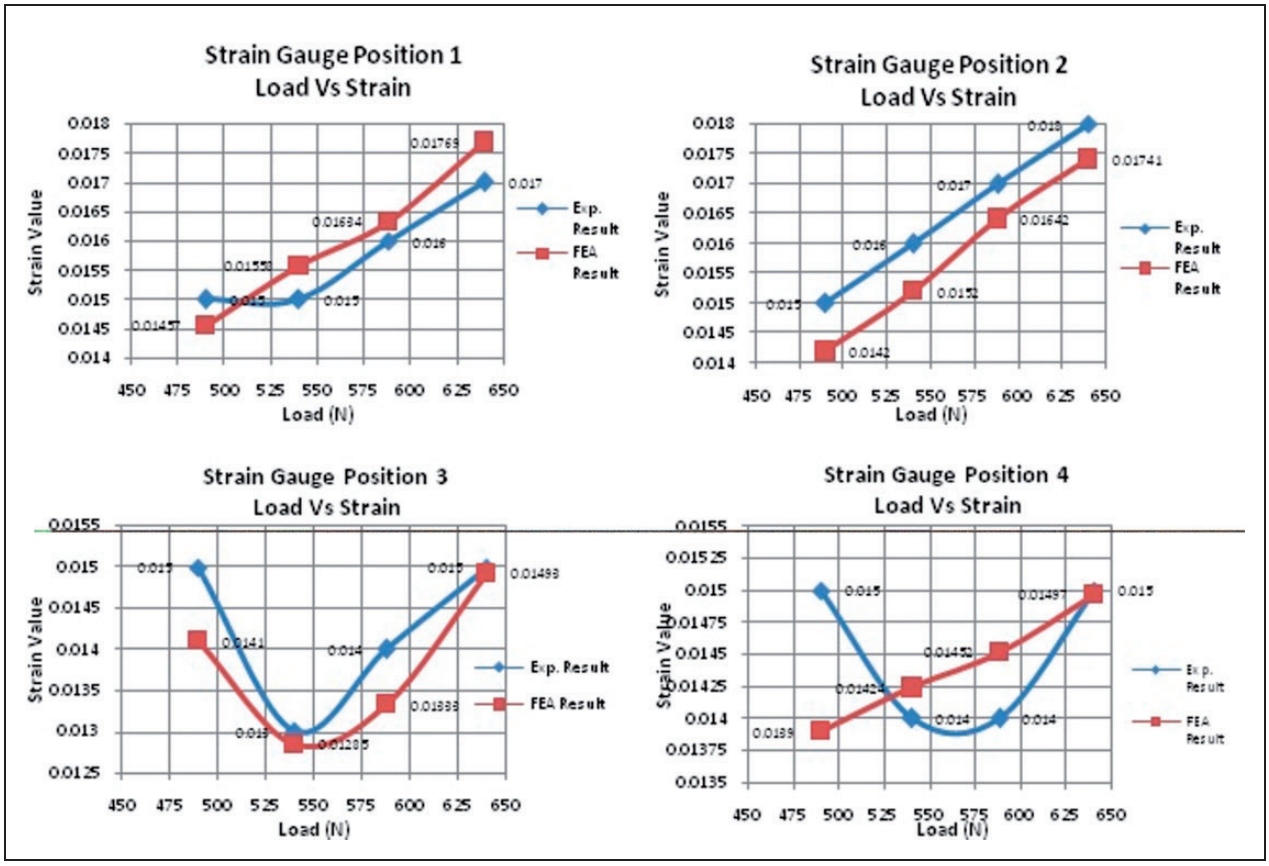


**Figure 8.** Comparatives between strain value for experimental and FEA results based on strain gauge positions.

position 2, as the loads were increased for the experimental and FE analysis, strain also increased, and the errors calculated are very less.

For strain gauge position 3, strain values decreased till 540 N for both experimental and FEA and then increased to 640 N. The errors obtained are very meager. For strain gauge position 4, the experimental results showed decrease in strain values till 540 N and then increased, whereas in FEA results, as the loads were increased, strain also increased, and the errors are less for FEA when compared with the experimental values.

It is obvious from FEA that the neck inferior and neck superior have maximum stress and strain compared to other positions. FE analysis of the stress and strain behavior with different loads were comparable with the experimental analysis for the femur bone.

In general, the errors obtained for stress and strain correlation for FE analysis are around 5% when compared with the experimental values.

## Conclusion

The experimental result of femur bone shows that the stress and strain value for four locations in femur bone was studied earlier. Material properties and boundary conditions are initially applied before the different load on the femur bone under static condition. The different loads applied on the femur bones are 490 N (50 kg), 540 N (55 kg), 588 N (60 kg), and 640 N (65 kg) in the experiment, and results were obtained. The loads applied to the femoral head and medial condyle and strain gauge position 1, 2, 3, and 4 give the values of stress and strain, and the other end of femur bone was fixed in all degrees of freedom. The stress and strains predicted by FE models correlate with the experimental results. The stress and strains are measured from the experiment of four positions of the strain gauges in which the force is applied and subsequently compared to the FE stress and strains of the same positions. The strain value error obtained is lesser for neck inferior and neck superior and higher for shaft lateral and shaft medial. The neck inferior and neck superior position has the higher stress value when compared with shaft lateral and shaft medial. The error obtained when the results of FEA are around 5%. The highest strain observed on the neck side of the femur and the results imply that higher weight leads to higher total displacement. Experiments on the femur bones may be avoided because the results obtained from FEA are much better when compared with the experimental results. The FEA result of stress and strain value is closely adhered with the experimental results and found only minimum deviation between them. This works proved that the FEA technique is much suited to find out stress and strain value in real femur bone rather than any experimental work. It is very useful for the orthopedic surgeons and medical engineers.

### Declaration of Conflicting Interests

The author(s) declared no potential conflicts of interest with respect to the research, authorship, and/or publication of this article.

### Funding

The author(s) received no financial support for the research, authorship, and/or publication of this article.

### ORCID iD

S Mathukumar https://orcid.org/0000-0003-4147-9620

### References

1. Enns-Bray WS, Ariza O, Gilchrist S, et al. Morphology based anisotropic finite element models of the proximal femur validated with experimental data. *Med Eng Phys* 2016; 38: 1339–1347.
2. Schileo E, Dall Ara E, Taddei F, et al. An accurate estimation of bone density improves the accuracy of subject specific finite element models. *J Biomech* 2008; 4: 2483–2491.
3. Francis A and Kumar V. Computational modeling of human femur using CT data for finite element analysis. *Int J Eng Res Technol*, November 2013; DOI: 10.1007/978-81-322-0970-6_8.
4. Enns-Bray WS, Owoc JS and Nishiyama KK. Mapping anisotropy of the proximal femur for enhanced image based finite element analysis. *J Biomech* 2014; 47: 3272–3278.
5. Luisier B, Dall Ara E and Pahr D. Orthotropic HR-pQCT-based FE models improve strength predictions for stance, but not for side-way fall loading compared to isotropic QCT-based FE models of human femurs. *J Mech Behav Biomed Mater* 2014; 32: 287–299.
6. Marangalou J, Ito K and van Rietbergen B. A new approach to determine the accuracy of morphology elasticity relationships in continuum FE analyses of human proximal femur. *J Biomech* 2012; 45: 2884–2892.
7. San Antonio T, Ciaccia M and Müller-Karger C. Orientation of orthotropic material properties in a femur FE model: a method based on the principal stresses directions. *Med Eng Phys* 2012; 34: 914–919.
8. Trabelsi N and Yosibash Z. Patient-specific finite-element analyses of the proximal femur with orthotropic material properties validated by experiments. *J Biomech Eng* 2011; 133: 061001.
9. Peng L, Bai J and Zeng X. Comparison of isotropic and orthotropic material property assignments on femoral finite element models under two loading conditions. *Med Eng Phys* 2006; 28: 227–233.
10. Lekadir K, Noble C, Hazrati-Marangalou J, et al. Patient specific biomechanical modeling of bone strength using statistically derived fabric tensors. *Ann Biomed Eng* 2016; 44: 234–246.
11. Larsson D, Luisier B, Kersh ME, et al. Assessment of transverse isotropy in clinical level CT images of trabecular bone using the gradient structure tensor. *Ann Biomed Eng* 2014; 42: 950–959.
12. Prendergast PJ. Finite element models in tissue mechanics and orthopedic implant design. *Clin Biomech* 1997; 12(6): 343–366.

13. Pfeiler TW, Lalush DS and Loboa EG. Semiautomated finite element mesh generation methods for a long bone. *Comput Meth Prog Biomed* 2007; 85: 196–202.
14. Taddei F, Pancanti A and Viceconti M. An improved method for the automatic mapping of computed tomography numbers onto finite element models. *Med Eng Phys* 2004; 26: 61–69.
15. Taddei F, Schileo E and Helgason B. The material mapping strategy influences the accuracy of CT based finite element models of bones: an evaluation against experimental measurements. *Med Eng Phys* 2007; 29: 973–979.
16. Helgason B, Perilli E and Schileo E. Mathematical relationships between bone density and mechanical properties: a literature review. *Clin Biomech* 2008; 23(2): 135–146.
17. Helgason B, Taddei F and Palsson H. A modified method for assigning material propertied to FE models of bones. *Med Eng Phys* 2008; 30(4): 444–453.
18. Edidin A, Taylor D and Bartel DL. Automatic assignment of bone moduli from CT data: a 3D finite element study. In: *Proceedings of the 37th annual meeting of the orthopaedic research society*, Anaheim, California, 1991, p.491.
19. Merz B, Niedere P and Muller R. Automated finite element analysis of excised human femora based on precision-QCT. *J Biomech Eng* 1996; 118(3): 387–390.
20. Jadhav MV and Gambhire VR. Experimental analysis of stress in real (preserved) intact proximal human femur (thigh) bone under static load. *IJATES* 2015; 3(1): 1179–1187.
21. Schileo E, Taddei F and Cristofolini L. Subject specific finite element models implementing a maximum principal strain criterion are able to estimate failure risk and fracture location on human femurs tested in vitro. *J Biomech* 2008; 41: 356–367.
22. Yosibash Z, Trabelsi N and Milgrom C. Reliable simulations of the human proximal femur by high order finite element analysis validated by experimental observations. *J Biomech* 2007; 40(16): 3688–3699.
23. Trabelsi N, Yosibash Z and Milgrom C. Validation of subject- specific automated p-FE analysis of the proximal femur. *J Biomech* 2009; 42(3): 234–241.
24. Jacobs CR, Simo JC and Beaupre GS. Adaptive bone remodeling incorporating simultaneous density and anisotropy considerations. *J Biomech* 1997; 30: 603–613.
25. Youn K, Park MS and Lee J. Iterative approach for 3D reconstruction of the femur from un-calibrated 2D radiographic images. *Med Eng Phys* 2017; 50: 89–95.
26. Conlisk N and Howie CR. Computational modeling of motion at the bone implant interface after total knee arthroplasty: the role of implant design and surgical fit. *Knee* 2017; 24(5): 994–1005.
27. Marco M, Giner E and Larraínzar-Garijo R. Modelling of femur fracture using finite element procedures. *Eng Fract Mech* 2018; 0013–7944.
28. Peleg E, Beek M and Joskowicz L. Patient specific quantitative analysis of fracture fixation in the proximal femur implementing principal strain ratios. Method and experimental validation. *J Biomech* 2010; 43: 2684–2688.
29. Kim J-T, Jung C-H and Shen QH. Mechanical effect of different implant CCD angles on the fracture surface after fixation of an unstable intertrochanteric fracture: a finite element analysis. *Asian J Surg*. Epub ahead of print 20 February 2019. DOI: 10.1016/j.asjsur.2019.01.008.
30. Lopes VMM, Neto MA, Amaro AM, et al. FE and experimental study on how the cortex material properties of synthetic femurs affect strain levels. *Med Phys Eng* 2017; 46: 96–109.